Cancer Cell International

RESEARCH Open Access

Low NDFIP1-driven metabolic alterations in CD8+T cells: implications for immune evasion and therapy resistance in HNSC

Jun Wan[1], YiBo Zhou[1], Dan Xie[1], Zhi Chen[1], Dan Yang[1], Yi Tang[1], YaFang Zuo[1], Dingan Luo[3*] and Lu Wang[2*]

Abstract

Head and neck squamous cell carcinoma (HNSC) is an aggressive malignancy often resistant to therapy, especially in advanced stages. Metabolic reprogramming, marked by shifts in glycolysis and oxidative phosphorylation (OXPHOS), is crucial for tumor progression and immune evasion. This study provided a single-cell transcriptomic map of 53,660 CD8+T cells from primary and metastatic HNSC samples, identifying 11 distinct CD8+T cell subsets. Notably, PDCD1+CD8+ T cells were enriched in metastatic sites, exhibiting heightened expression of PD-1 and LAG3, as well as activation of JAK-STAT and PD-L1/PD-1 signaling pathways. A focused analysis revealed five key driver genes-PLS3, NDFIP1, MED15, JCHAIN, and FTH1-associated with prognosis, as identified using machine learning models. NDFIP1 was downregulated in various tumors, including HNSC, and its expression correlated strongly with increased CD8+T cell infiltration, OXPHOS activity, and enhanced immune pathways. Patients with higher NDFIP1 expression showed better survival outcomes and were linked to an immune subtype characterized by robust CD8+T cell activity and IFN-γ signaling. Thus, NDFIP1 emerges as a crucial biomarker for predicting immunotherapy response and offers insight into targeting metabolic pathways in cancer treatment, as its downregulation is associated with immune evasion and worse clinical outcomes.

Keywords Head and neck squamous cell carcinoma, NDFIP1, CD8+T cells, Oxidative phosphorylation, Immunotherapy

Introduction

Head and neck squamous cell carcinoma (HNSC) is a common and aggressive tumor that primarily originates from the mucosal epithelium of the head and neck. Its development is closely linked to smoking, alcohol consumption, and human papillomavirus (HPV) infection [1]. Despite advances in surgery, radiotherapy, chemotherapy, and immunotherapy, the prognosis for advanced HNSC remains poor due to limited therapeutic response and resistance [2, 3]. Disruptions in energy metabolism are recognized as a significant factor affecting treatment efficacy, contributing to tumor progression and playing a crucial role in immune evasion, which further complicates treatment.

*Correspondence:
Dingan Luo
18707493640@163.com
Lu Wang
wl76098797@163.com
[1]Department of Otolaryngology Head and Neck Surgery, Changsha Hospital of Traditional Chinese Medicine (Changsha Eighth Hospital, 22 Xingsha Avenue, Changsha 410100, Hunan, China
[2]Department of Otolaryngology Head and Neck Surgery, Integrated Traditional Chinese and Western Medicine Second Hospital Affiliated with Hunan University of Chinese Medicine, 67 Beizheng Middle Road, Liuyang, 410300, Hunan, China
[3]Xiangya Hospital of Central South University, 87 Xiangya Road, 410008 Changsha, China

The role of energy metabolism in tumor biology has gained increasing attention, particularly in HNSC and other cancers [4]. Cancer cells undergo metabolic reprogramming to meet the demands of rapid proliferation, which is characterized by enhanced glycolysis and altered mitochondrial function. For instance, the glycolysis and Warburg effect commonly observed in HNSC lead to lactate accumulation and acidification of the tumor microenvironment, which suppresses local immune responses [5, 6]. Tumors exhibit varying metabolic profiles, with some relying on oxidative phosphorylation (OXPHOS) for sustained growth. In particular, CD8 + T cell function is significantly affected by metabolic dysregulation within the tumor microenvironment, where alterations in OXPHOS can result in immune suppression, allowing tumor cells to evade immune surveillance and proliferate unchecked [7, 8].

In cancer research, the role of NDFIP1 (Nedd4 family interacting protein 1) has garnered increasing attention. NDFIP1 plays a crucial role in cellular protein transport and signaling regulation, but its specific function in cancer remains underexplored [9, 10]. There is currently limited research on the relationship between NDFIP1 and oxidative phosphorylation, especially regarding its role in CD8 + T cells and tumor immunity. Investigating NDFIP1's involvement in tumor metabolism regulation, particularly its effects on OXPHOS and immune cell function, could reveal potential mechanisms of immune evasion and provide new therapeutic targets to improve immunotherapy efficacy in HNSC and other cancers.

In this study, we generated a single-cell transcriptomic atlas of 53,660 CD8 + T cells, revealing the complex and diverse transcriptional profiles of these cells. We identified 11 distinct cell states, with CCL5-expressing effector CD8 + T cells predominating, alongside stress-induced T cells expressing heat shock proteins. Notably, PDCD1 + CD8+ T cells were found to exhibit unique immune phenotypes and metabolic characteristics, promoting tumor metastasis and suppressing the cytotoxic function of CD8 + T cells. Through multimodal data analysis-including bulk transcriptomics, single-cell transcriptomics, spatial transcriptomics, and proteomics-we explored the potential mechanisms of NDFIP1 in the PDCD1 + CD8+ T cell subset. These findings highlight the potential of targeting NDFIP1 in precision medicine and suggest promising avenues for developing innovative immunotherapies for HNSC.

Materials and methods

scRNA-seq cohorts

HNSC specimens were collected from surgical patients at Changsha Hospital of Traditional Chinese Medicine. The resected specimens were immediately collected and subjected to pathological diagnosis. Informed consent was obtained from all patients, and the study was approved by the Clinical Research Ethics Committee of Changsha Hospital of Traditional Chinese Medicine.

To identify specific CD8 + T cell subpopulations and their functional roles in HNSC, single-cell RNA sequencing data were obtained from publicly available datasets, including both primary and metastatic tumor samples. For scRNA-seq data, single cells were first screened for expression of each gene in at least 3 cells, with at least 250 genes expressed per cell. The ratio of mitochondria to rRNA was then evaluated using the PercentageFeatureSet function in the Seurat R package. Single cells were further screened by setting each cell to express at least 9,000 genes with a UMI > 200. Finally, a total of 53,660 cells remained.

RNA-seq cohorts

In addition to the scRNA-seq cohort, transcriptomic data and clinical information were available for three RNA-seq cohort samples (TCGA_HNSC, GSE65858, GSE41613, GSE117973). The TCGA-HNSCC cohort predominantly comprises head and neck squamous cell carcinoma samples. HPV status was obtained from TCGA clinical annotations. GSE117973 represents the HIPO-HNC cohort and comprises primary HNSCC tumor samples profiled using multi-omics approaches, including DNA methylation and gene expression analysis. GSE41613 contains gene expression data from 97 patients with HPV-negative oral squamous cell carcinoma (OSCC). GSE65858 includes gene expression profiles from a large HNSCC cohort with well-annotated HPV16 DNA and RNA (E6*I) status; after quality control, 270 primary tumor samples were retained. Model training and validation were carried out with the "Mime" R package, using the differential genes identified earlier. Model performance was evaluated using receiver operating characteristic (ROC) curves, and area under the curve (AUC) values were calculated to assess predictive power.

Spatial transcriptome analysis

Spatial transcriptomics data were utilized to analyze the spatial distribution of CD8 + T cells in tumor microenvironments. Seurat's SpatialDimPlot function was employed to visualize the cellular composition in specific tumor regions. To assess the relationship between gene expression and cell type abundance, Spearman correlation analyses were performed using the linkET package, enabling the visualization of gene expression across various tumor microregions.

Functional enrichment analysis

KEGG enrichment analysis was performed using the clusterProfiler package to assess the functional pathways involved. The CancerSEA database was utilized to classify

the functional states of tumor cells. To evaluate pathway activity, the z-score algorithm proposed by Lee et al. was employed, integrating the expression levels of characteristic genes. The GSVA package in R was used to compute combined z-scores for functional state gene sets, which were subsequently standardized to derive gene set scores [11]. RBN RPPA data were centered on the median and normalized by the standard deviation of all samples for each component to determine relative protein levels. Pathway scores were then calculated by summing the relative protein levels of the positive regulatory components in each pathway and subtracting the protein levels of the negative regulatory components [12]. Simpler software packages use PROGENy to calculate pathway scores. Pathway-specific characterization was obtained by pathway perturbation experiments, which assessed changes in gene expression following pathway disruption. A linear regression model was used to fit the genes affected by pathway perturbation. Pathway-specific features and gene expression data were then used to infer pathway signaling activity.

Basic experimental verification

CD8 + T cells were negatively selected from peripheral blood (schbio, PBMNC010C) using the CD8a + T cell isolation kit from Miltenyi Biotec. After isolation, CD8 + T cells were activated with 2 μg/mL αCD3 and 2 μg/mL αCD28 coated on plates, and cultured in RPMI-1640 medium supplemented with 10% heat-inactivated FBS and 1% penicillin-streptomycin. The cells were harvested and incubated with 100 μM DHE for 30 min in the dark at 37 ∘C. Then, the cells were washed three times with 0.01 M PBS. The fluorescence signals were analyzed by flow cytometry.

Total RNA was isolated using Direct-zol RNA MiniPrep Kit (Genesee Scientific, 11–330). For multiple immunofluorescences, experiments were conducted under the conditions of previous literature [13]. The qPCR was performed using PerfeCTa® SYBR® Green FastMix (QuantaBio, 101414-270) on a Roche LightCycler 480 (Roche) detection system according to the manufacturer's instruction. The following primers were used:

NDFIP1 (F: GAGTCTGGAGAACCTGAACAGG, R:GGCTTTGGAAACCCAGACTCATC); PIK3CA (F: GAAGCACCTGAATAGGCAAGTCG, R:GAGCATCCATGAAATCTGGTCGC); AKT1 (F: TGGACTACCTGCACTCGGAGAA, R:GTGCCGCAAAAGGTCTTCATGG); COX4I1 (F: TCGGTTTCACCGCGCTCGTTAT, R:TGTCCAGCATCCTCTTGGTCTG); PGC1A (F: CCAAAGGATGCGCTCTCGTTCA, R: CGGTGTCTGTAGTGGCTTGACT); TNFRSF9 (F: TCTTCCTCACGCTCCGTTTCTC, R:TGGAAATCGGCAGCTACAGCCA); GZMB (F: CGACAGTACCATTGAGTTGTGCG, R: TTCGTCCATAGGAGACAATGCCC); IFNG (F: GAGTGTGGAGACCATCAAGGAAG, R: TGCTTTGCGTTGGACATTCAAGTC); PD-1 (F: AAGGCGCAGATCAAAGAGAGCC, R:CAACCACCAGGGTTTGGAACTG).

Statistical analysis

All statistical analyses were performed using R software (version 4.1.0). The Wilcoxon test was used to analyze differences between two groups, while the Kruskal-Wallis's test was applied to analyze differences among more than two groups. Survival analyses were performed using Kaplan-Meier plots and the log-rank test to evaluate the prognostic significance of key genes, including NDFIP1. Cox proportional hazards regression was employed for multivariate survival analysis. Statistical significance was defined as a p-value < 0.05, unless otherwise noted.

Results

Overview of CD8 T cell subsets in HNSC

To uncover specific subpopulations and potential functions of CD8 + T cells in HNSC, we generated a single-cell transcriptomic map consisting of 53,660 CD8 + T cells from both primary and metastatic samples. CD8 + T cells from primary and metastatic sources accounted for 44% and 56% of the total population, respectively. We clustered these cells to decode their transcriptional signals, identifying 11 stable clusters, each characterized by distinct signature genes (Fig. 1A). The CCL5 + CD8+ T cell cluster was the most abundant (Fig. 1B), with its proportion reduced in metastatic lesions compared to primary lesions (Fig. 1C). These cells primarily secrete effector molecules such as CCL5 and GZMH (Fig. 1D) and show enrichment in MHC class I molecules (Fig. 1E) and cytokine-cytokine receptor interactions (Fig. 1F), which are typically associated with effector T cell functions [14]. PDCD1 + CD8+ T cells were more prevalent in metastatic lesions compared to primary tumors, expressing high levels of PDCD1 and LAG3, and were enriched for JAK-STAT and PD-L1/PD-1 signaling pathways. The TSTR subset, characterized by a stress-response state and high expression of heat shock proteins HSPA1A and HSPA1B, was enriched in NF-κB and PPAR signaling pathways. To further investigate the PDCD1 + CD8+ T cell subset, we performed a cell-cell communication analysis, revealing interactions between PDCD1 + CD8+ T cells and both CCL5 + and CXCL13 + CD8+ T cells (Fig. 1G). In summary, our CD8 + T cell map not only captures well-known CD8 + T cell subtypes but also identifies previously uncharacterized subsets.

Identification of key driver genes in PDCD1 + CD8 T cells

To further explore the signature genes of PDCD1 + CD8+ T cells, we analyzed the differential genes between metastatic and primary lesions within the PDCD1 + CD8+ T cell subset (Figure S1A), as well as the differential

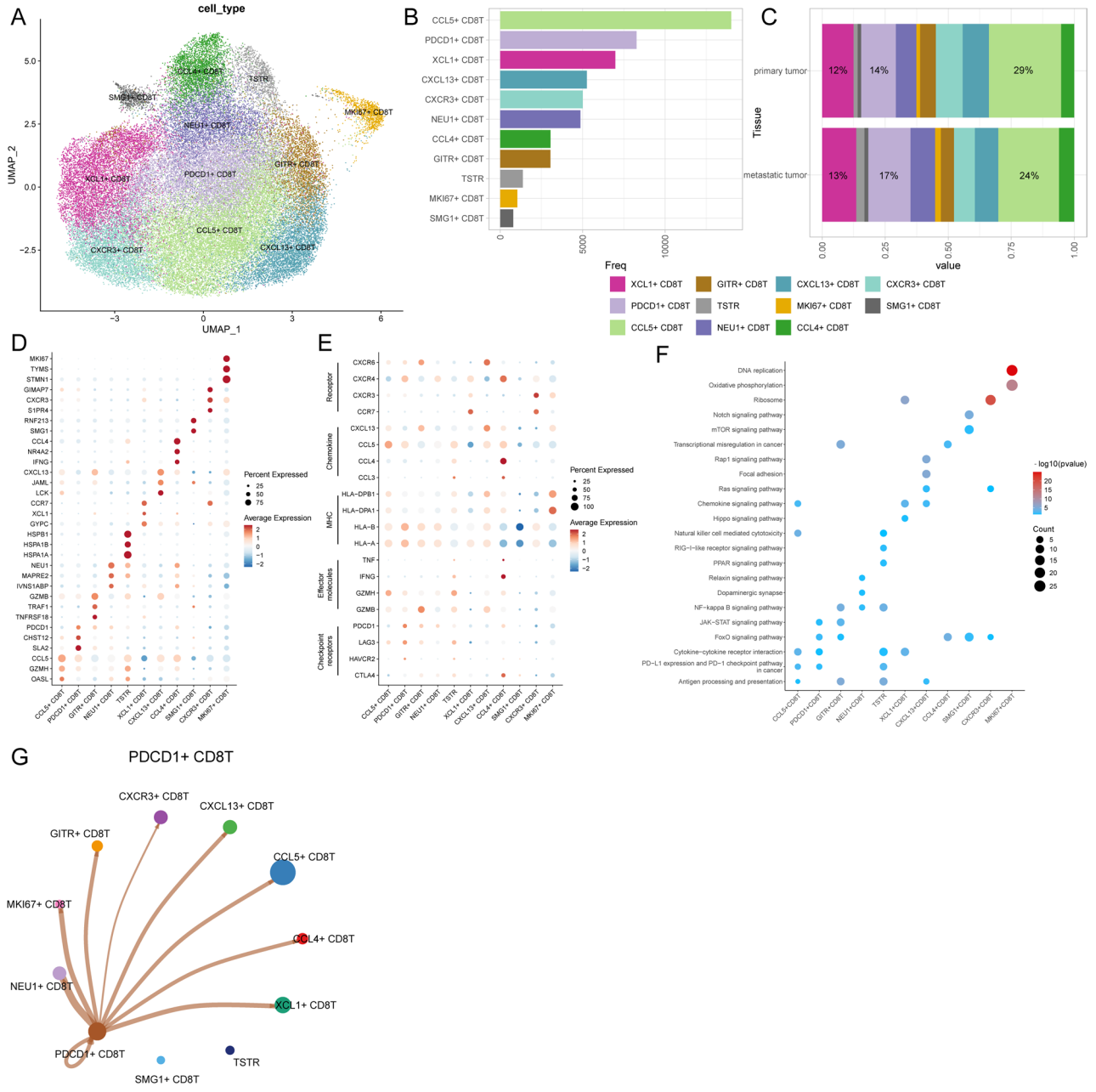

Fig. 1 Overview of CD8 T Cell Subsets in HNSC. **a** UMAP visualization of CD8 + T cell subsets. **b**-**c** The number and proportion of CD8 T cells. Numerical values indicate the mean proportion of dominant cell populations. Due to the compositional nature of the data and the lack of independent biological replicates at the cell-frequency level, formal statistical testing was not performed for these proportions. **d** Gene expression heatmap in T cell subsets. **e** Expression profiles of differentially expressed cytokines, MHC, effector molecules, checkpoint receptors, and receptor. **f** Enriched pathways of each T cell subset. **g** Cell communication analysis of PDCD1 + CD8Tn in all cells. the diameter of each node represents the number of cells in the corresponding subset, and the edges between nodes indicate the relative communication strength between cell subsets

genes between PDCD1 + CD8+ T cells and other CD8⁺ T-cell subsets identified in the CD8⁺ T-cell subclustering analysis across all metastatic lesions (Figure S1B). We identified 1,230 shared genes (Figure S1C). To further narrow down the subset-specific genes, we constructed 117 prognostic models using the R package Mime1. The StepCox[backward] + Ridge model demonstrated strong predictive power for 5-year prognosis across multiple datasets, with an AUC of 0.865 in the training set (Fig. 2A). The ROC curve in Fig. 2B further illustrated the model's robust performance. Five genes-PLS3, NDFIP1, MED15, JCHAIN, and FTH1-were identified as critical drivers of HNSC progression across multiple models (Fig. 2C and D). Thus, through machine learning, we identified five key genes associated with PDCD1 + CD8+ T cell-driven metastasis in HNSC.

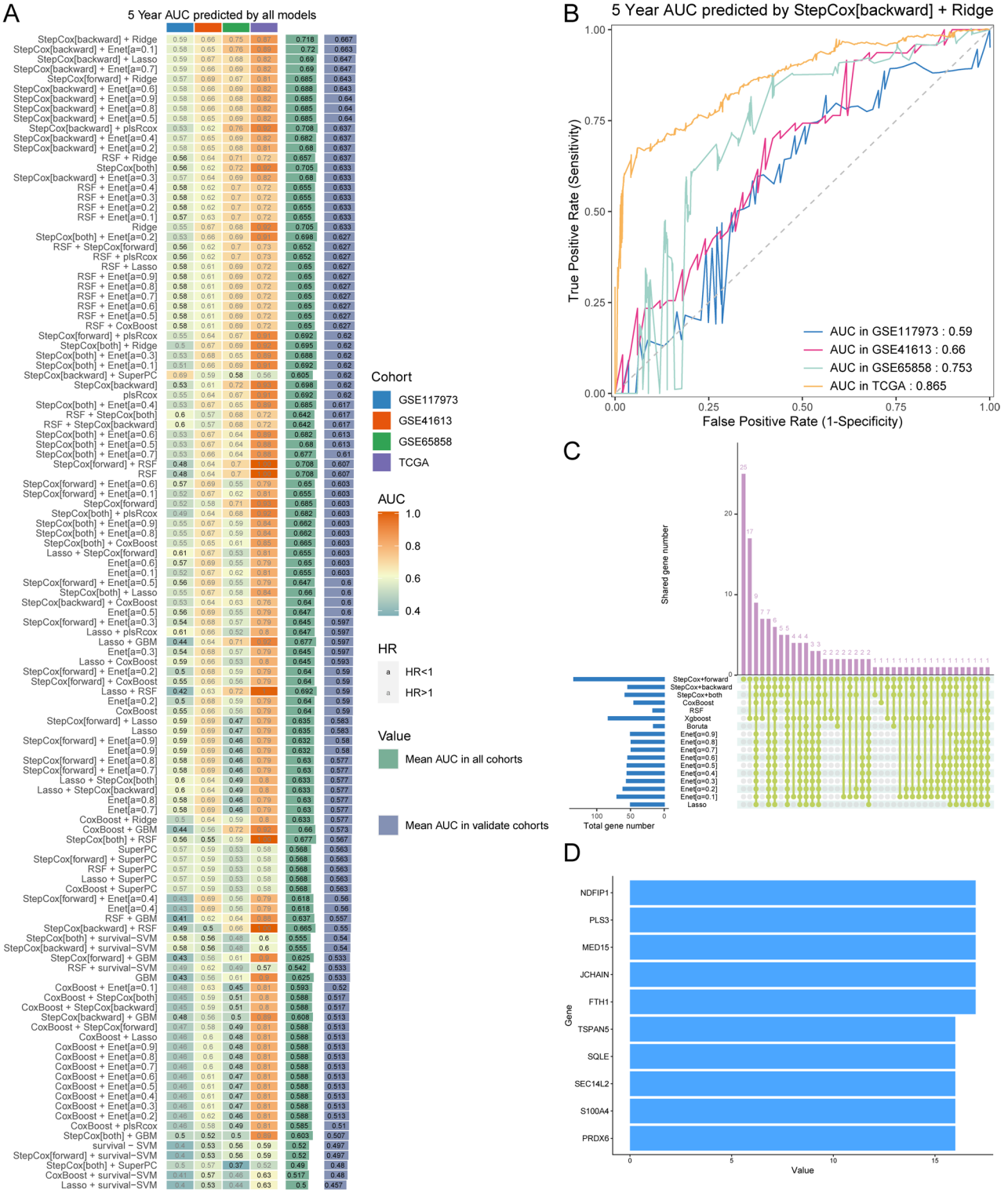

Fig. 2 Identification of key driver genes in PDCD1 + CD8 T Cells. (**a**) 117 machine learning models were used to predict the AUC of 5-year prognosis. (**b**) ROC curves for predicting 5-year outcomes using the StepCox[backward]+Ridge model. (**c**-**d**) Five genes-PLS3, NDFIP1, MED15, JCHAIN, and FTH1-were consistently identified as for HNSC across multiple models

Expression and prognostic analysis of NDFIP1 in pan cancer

To validate the metastasis-related genes in PDCD1 + CD8+ T cells, we conducted an in-depth analysis of PLS3, NDFIP1, MED15, JCHAIN, and FTH1. We found that NDFIP1 was downregulated in multiple tumor types, including HNSC, compared to normal tissues (Figure S2A). Analysis using the HPA database revealed that NDFIP1 and MED15 were predominantly expressed in CD8 + T cells (Fig. 3A, Figure S2B-S2E). NDFIP1 is likely a key gene in PDCD1 + CD8+ T cell-mediated metastasis in HNSC. To further investigate the function of NDFIP1, we performed pan-cancer analysis. In both paired and unpaired tests, NDFIP1 was significantly downregulated across various cancers, including HNSC ($p < 0.01$), and showed strong diagnostic potential (Fig. 3B). At the protein level, based on the human protein atlas database, NDFIP1 is lowly expressed in several tumors including HNSC (Fig. 3C). More importantly, patients with high NDFIP1 expression had better survival outcomes than those with low expression, with consistent results across multiple datasets (Fig. 3D).

Enrichment analysis of NDFIP1 in pan cancer and its relationship with immune cell infiltration

NDFIP1 was positively correlated with oxidative phosphorylation in several cancers, including HNSC. Through various CD8 + T cell infiltration analyses, we found that NDFIP1 was positively correlated with CD8 + T cell infiltration across multiple cancers, including HNSC (Fig. 4A). Moreover, based on deconvolution results, we calculated the predominant cell type in each microregion

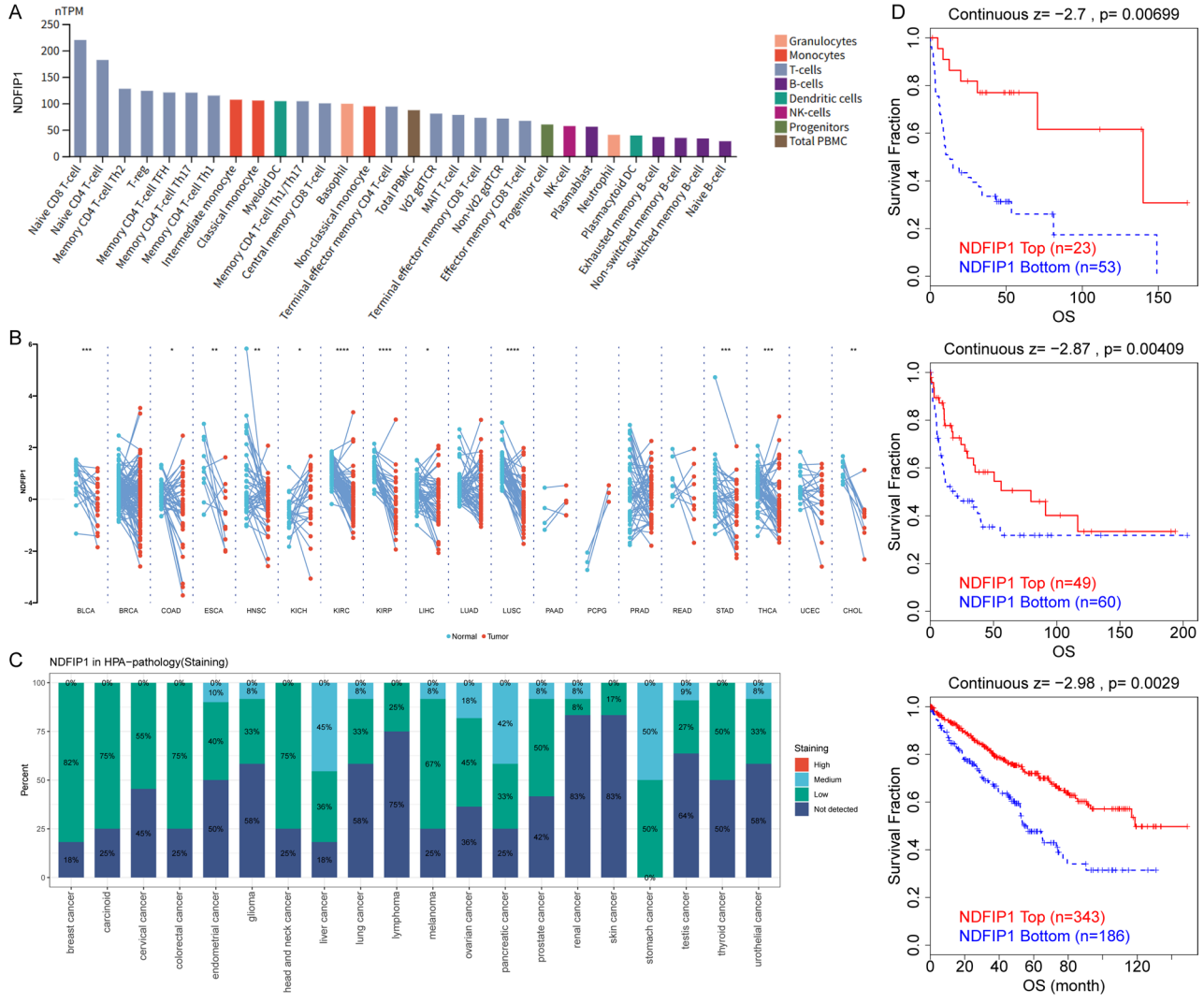

Fig. 3 Expression and prognostic analysis of NDFIP1 in pan cancer. (**a**) The transcript expression values (nTPM) resulting from the internal normalization pipeline are visualized for 29 blood cell types and total peripheral blood mononuclear cells (PBMC) from Monaco et al. (**b**) Differences in gene expression between tumor/normal groups (paired differential analysis). (**c**) Statistical analysis of The Human Protein Atlas immunohistochemical staining results. (**d**) The Kaplan-Meier survival analysis in GSE4475, GSE10885, and TCGA-Kidney

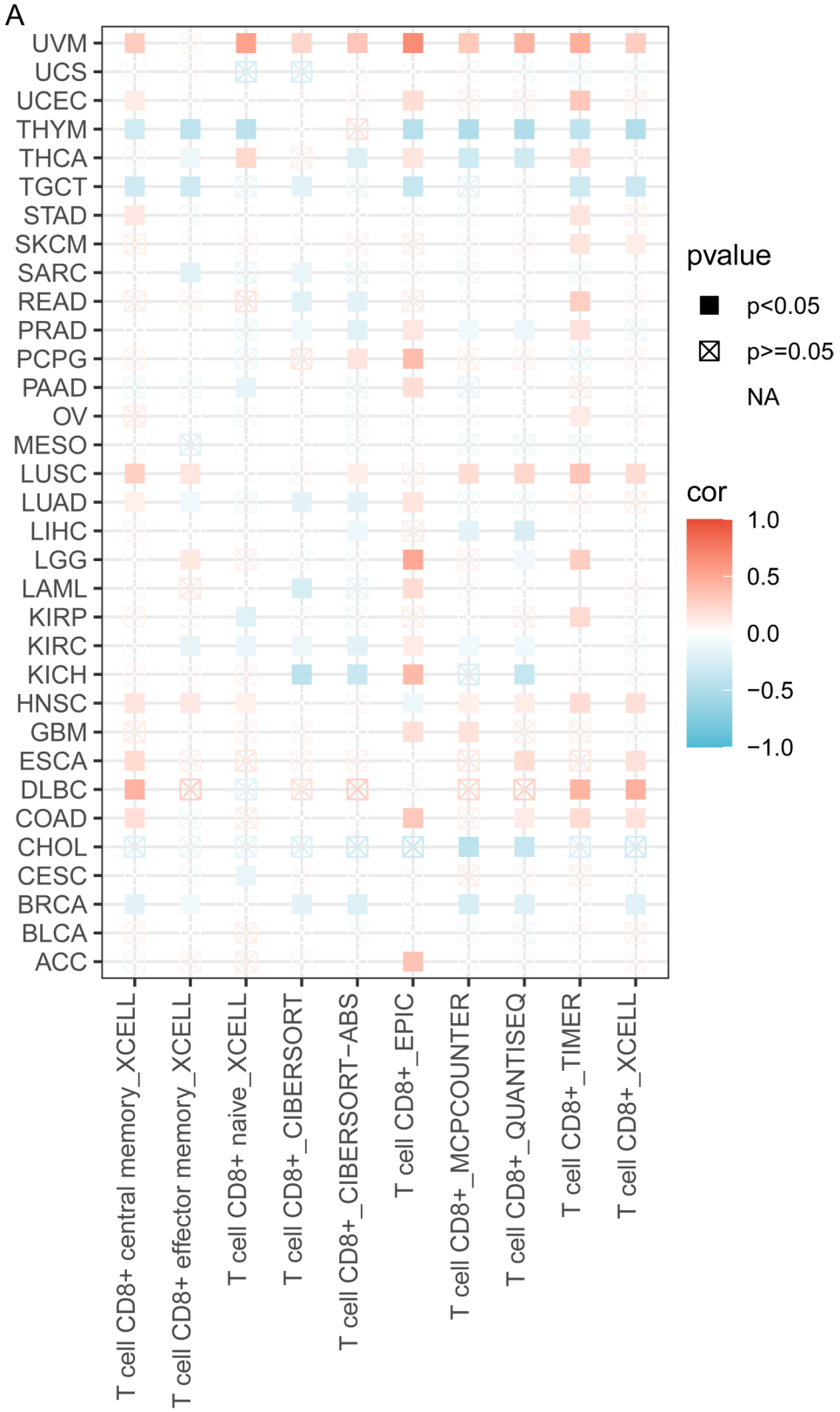

Fig. 4 Enrichment analysis of NDFIP1 in pan cancer. a Spearman correlation between NDFIP1 expression and immunoinfiltrating cells in pan-cancer

using spatial transcriptomics and visualized the maximum cell composition for each region using the SpatialDimPlot function from the Seurat package. We used Spearman correlation analysis to assess the relationships between cell content, gene signatures, and gene expression across all spots, and visualized the results using the linkET package. NDFIP1 was positively correlated with CD8 + T cells in GBM_UKF266-T-ST, HNSC_GSE181300, KIRC_GSE175540, LIHC_GSE203612, LUAD_GSE179572, and PCNSL_GSE203552 (Fig. 5A and F). In conclusion, NDFIP1 is a core gene associated with PDCD1 + CD8+ T cell-mediated metastasis in HNSC and other cancers. Its expression is negatively correlated with tumor cell cycle and invasion/metastasis, while positively correlated with CD8 + T cell infiltration and immune pathways, highlighting its crucial role in tumor immune regulation and prognosis prediction.

Enrichment analysis of NDFIP1 in HNSC

To further investigate the potential role of NDFIP1 in head and neck squamous cell carcinoma (HNSC), we conducted a detailed analysis. NDFIP1 was downregulated in tumors compared to normal tissues, as demonstrated in both paired and unpaired tests ($p < 0.01$) (Fig. 6A and B). In CD8 + T cells from multiple single-cell datasets, NDFIP1 was positively correlated with oxidative phosphorylation, the TNF signaling pathway, and the NF-kappa B signaling pathway (Fig. 6C). Using the "PROGENy" R package within the Easier package to calculate pathway scores, we found that the high NDFIP1 expression group was enriched for TNF and NF-kappa B signaling pathways, consistent with previous results (Fig. 6D, Figure S3A). Further analysis revealed a negative correlation between NDFIP1 expression and clinical stage, as well as with MKI67 expression (Fig. 6E), in line with prior findings.

The relationship between NDFIP1 and tumor immunity in HNSC

We performed KEGG enrichment analysis on metabolic gene sets across multiple HNSC transcriptome datasets. The results showed a positive correlation between NDFIP1 expression and oxidative phosphorylation, and a negative correlation with steroid hormone biosynthesis (Figure S4A). Further investigation revealed that NDFIP1 was significantly positively correlated with CYT, IFN-γ, and T cell-inflamed signatures ($p < 0.001$), suggesting its potential as a predictor for immune checkpoint

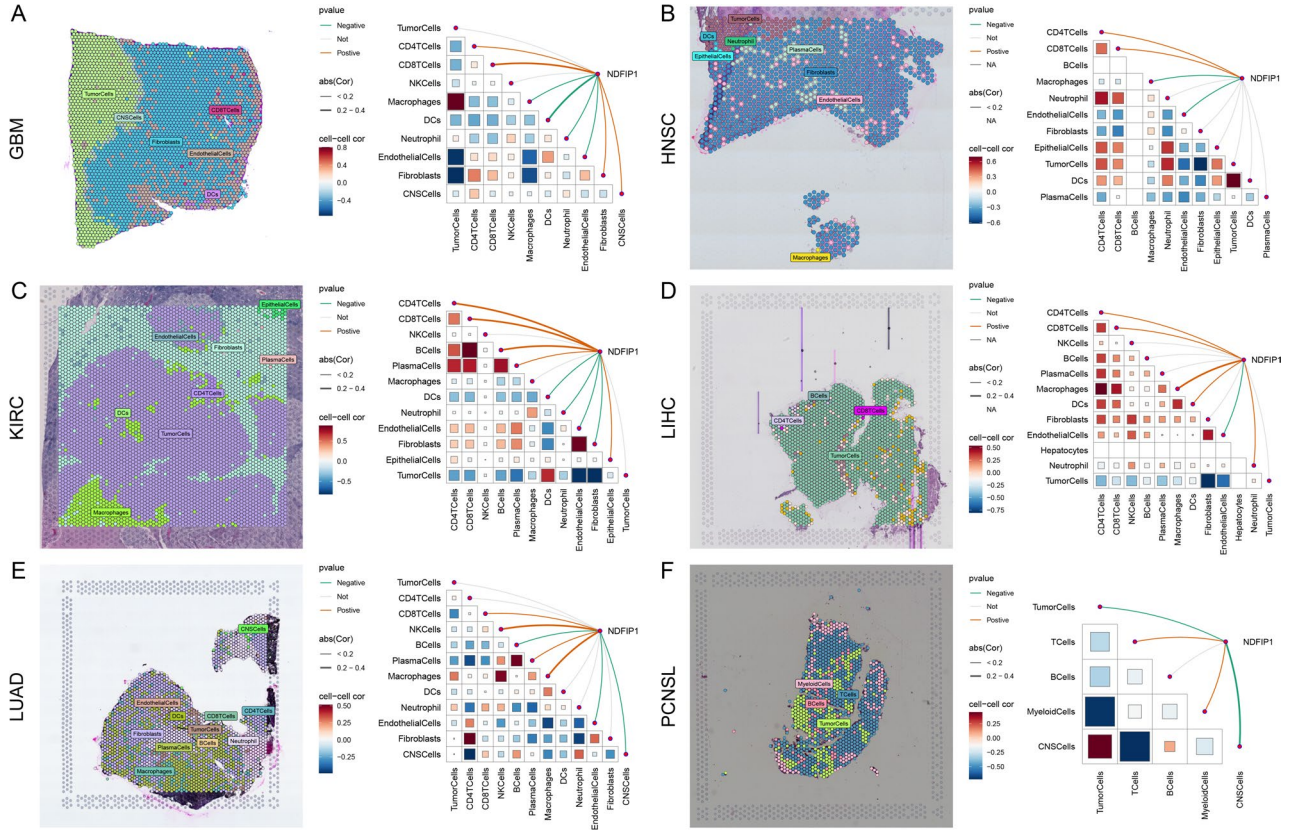

Fig. 5 The relationship between NDFIP1 and immune cell infiltration. a-f. Using the SpatialDimPlot function in the Seurat software package, the main cell types in each micro region were visualized. Spearman correlation analysis was then conducted to evaluate correlations between cell types across all spots, as well as between cell types and gene expression levels. Visualization was performed using the linkET package

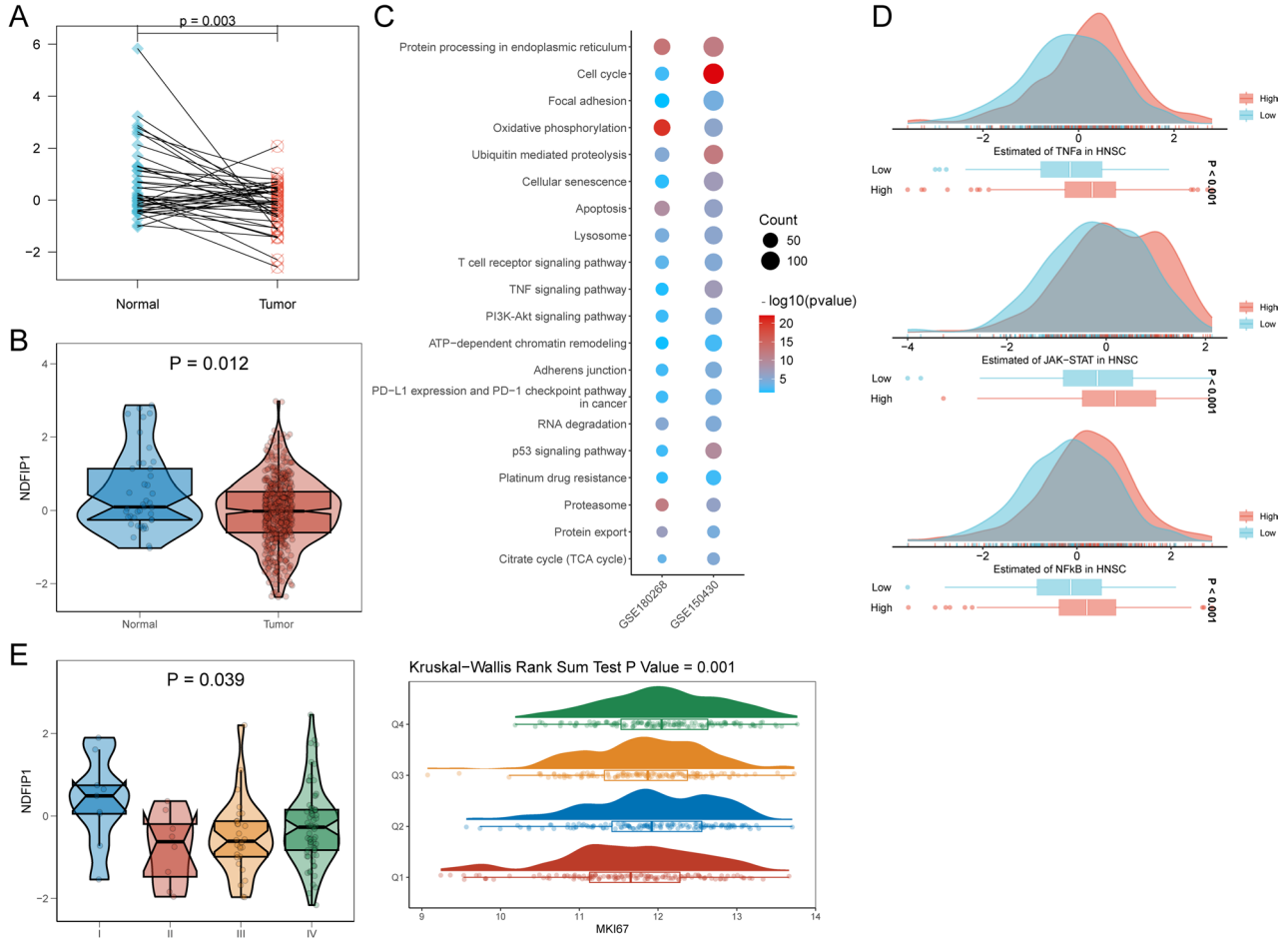

Fig. 6 Enrichment analysis of NDFIP1 in HNSC. (**a**) Differences in gene expression between tumor/normal groups (paired differential analysis). (**b**) Differential gene expression between the cancer/normal groups. (**c**) Enrichment analysis of differentially expressed genes of NDFIP1 in CD8 T cells with different single-cell data. (**d**) Difference of pathway score in high/low gene expression group. (**e**) Different NDFIP1 expression at different stages. The relationship between NDFIP1 and MKI67. Q1 represents the top 25% of samples with the highest expression, while Q4 represents the bottom 25% with the lowest expression

blockade (ICB) therapy response (Fig. 7A). Multiple algorithms confirmed a positive correlation between NDFIP1 expression and CD8 + T cell infiltration. Higher NDFIP1 expression was associated with increased CD8 + T cell infiltration (Fig. 7B). Across various datasets, NDFIP1 was positively correlated with cytotoxic T lymphocytes (CTLs) (Fig. 7C). Additionally, TIP (Tracking Tumor Immunophenotype), a meta-server that analyzes and visualizes cancer immune states and immune cell infiltration using RNA-seq or microarray data, showed that NDFIP1 was positively correlated with multiple steps of the cancer immunity cycle, including the release of cancer cell antigens (step 1), antigen presentation (step 2), immune cell transport to the tumor (step 4), and immune cell infiltration into the tumor (step 5) (Figure S4B). Collectively, NDFIP1 is downregulated in HNSC and influences oxidative phosphorylation, TNF, and NF-kappa B signaling pathways. Its strong association with immune-related features, particularly CD8 + T cell infiltration and antitumor immune responses, suggests a potential role in predicting immune therapy response and T cell exhaustion.

Bioinformatics and experimental validation of NDFIP1

To enhance the credibility of our results, we collected single-cell data from HNSC as extensively as possible for validation. The results showed that NDFIP1 was specifically highly expressed in CD8 + T cells across multiple datasets (Fig. 8A, D, G, J and M). Furthermore, in CD8 + T cells, NDFIP1 exhibited a significant positive correlation with the oxidative phosphorylation pathway ($p < 0.001$) (Fig. 8B, E, H, K and N). More importantly, NDFIP1 was positively correlated with TNFRSF9, GZMB, and IFNG and negatively correlated with PD-1 in CD8 + T cells (Fig. 8C, F, I, L and O, Figure S5A-S5E). Our analysis was based on RNA sequencing data previously generated by our research group (GSE64634). The results indicated that NDFIP1 was downregulated in

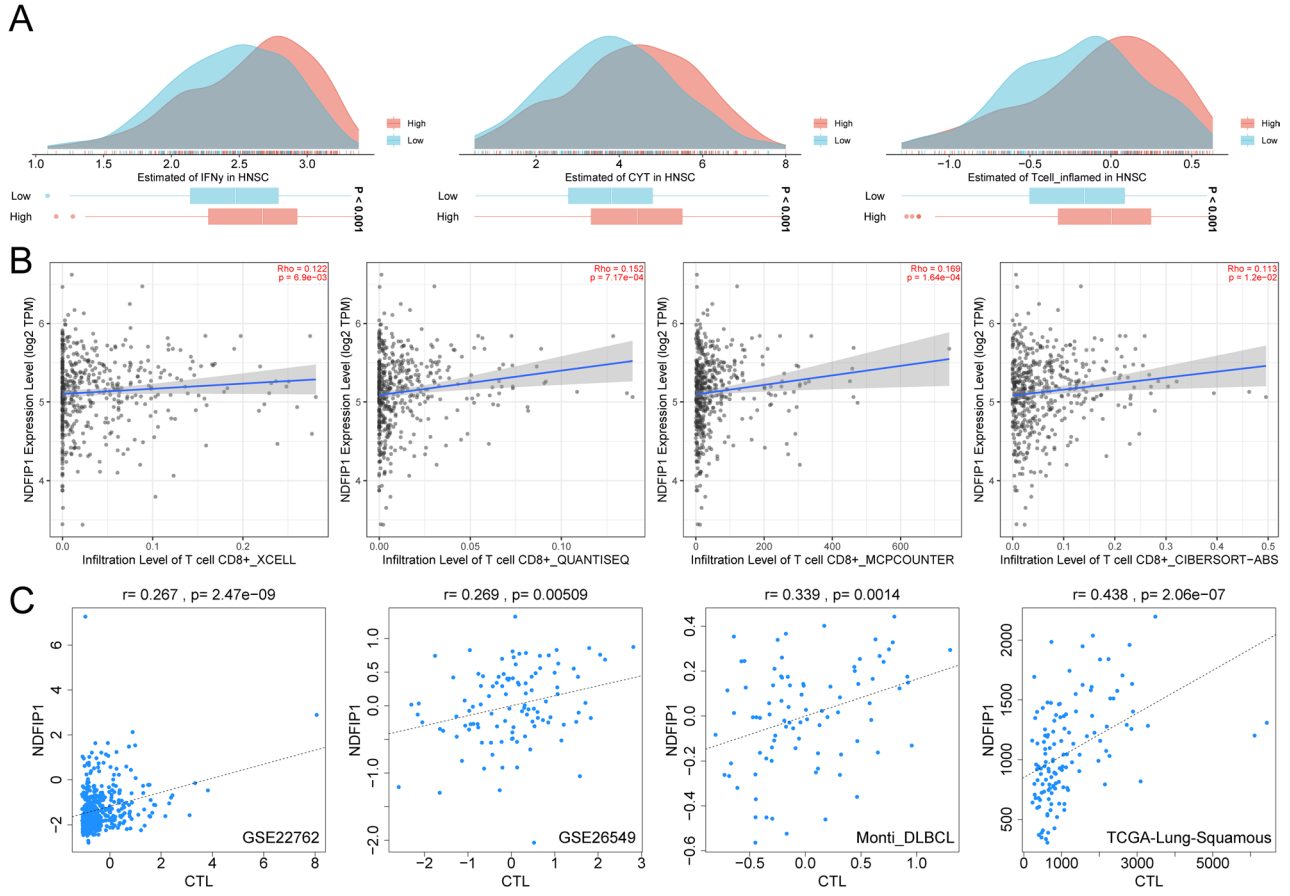

Fig. 7 The relationship between NDFIP1 and tumor immunity in HNSC. (**a**) Difference of pathway score in high/low NDFIP1 expression group. (**b**) Various immune cell infiltration algorithms reveal the relationship between NDFIP1 and CD8 T cell infiltration. (**c**) Correlation between NDFIP1 and CTLs in GSE22762, GSE26549, Monti_DLBCL, and TCGA-Lung-Squamous

tumors. Immune cell infiltration analysis using CIBERSORT revealed a positive correlation between NDFIP1 and CD8 + T cells, consistent with our prior findings (Figure S5F).

To further investigate the function of NDFIP1 in CD8 T cells, we knocked down NDFIP1 using siRNA (Fig. 9A). The results showed that the knockdown of NDFIP1 downregulated the expression levels of PIK3CA, AKT1, COXIV, and PGC-1α (Fig. 9B). Additionally, we evaluated changes in reactive oxygen species (ROS) levels, which are commonly regarded as an important metabolic marker of OXPHOS activity, using flow cytometry. Our analysis shows that knocking down NDFIP1 significantly reduces ROS production in CD8 + T cells ($p < 0.01$) (Fig. 9C). To investigate the regulatory effects of NDFIP1 on CD8 + T-cell function, we isolated CD8 + T cells from mouse spleens and activated them with CD3/CD28 antibodies to simulate T-cell activation during immune responses. qPCR analysis showed that the knockdown of NDFIP1 led to a decrease in the expression of activation markers such as GZMB, IFN-γ, and TNFRSF9 in CD8 + T cells, while exhaustion markers like PD-1 were significantly upregulated ($p < 0.01$) (Fig. 9D). Flow cytometry further confirmed these findings. Knockdown of NDFIP1 in CD8 + T cells showed a decrease in the expression levels of GZMB, IFN-γ, and TNFRSF9, while the expression of PD-1 was markedly increased (Fig. 9E).

The immunotherapeutic predictive potential of NDFIP1

To further explore the mechanisms by which NDFIP1 regulates tumor immunity, we performed differential gene expression analysis on PDCD1 + CD8+ T cells in single-cell data from GSE180268, as well as all CD8 + T cells in data from GSE150430, based on NDFIP1 expression levels (Figure S6A-S6C). Survival analysis based on NDFIP1 and TNFRSF9 expression showed that the group with low expression of both NDFIP1 and TNFRSF9 had worse prognosis compared to the group with high expression of both genes (Figure S6D). Previous findings indicated that NDFIP1 plays a key role in antitumor immunity in HNSC by regulating oxidative phosphorylation pathways. Further analysis revealed that in multiple animal models, NDFIP1 was upregulated in the effective immune therapy group (Fig. 10A), and oxidative

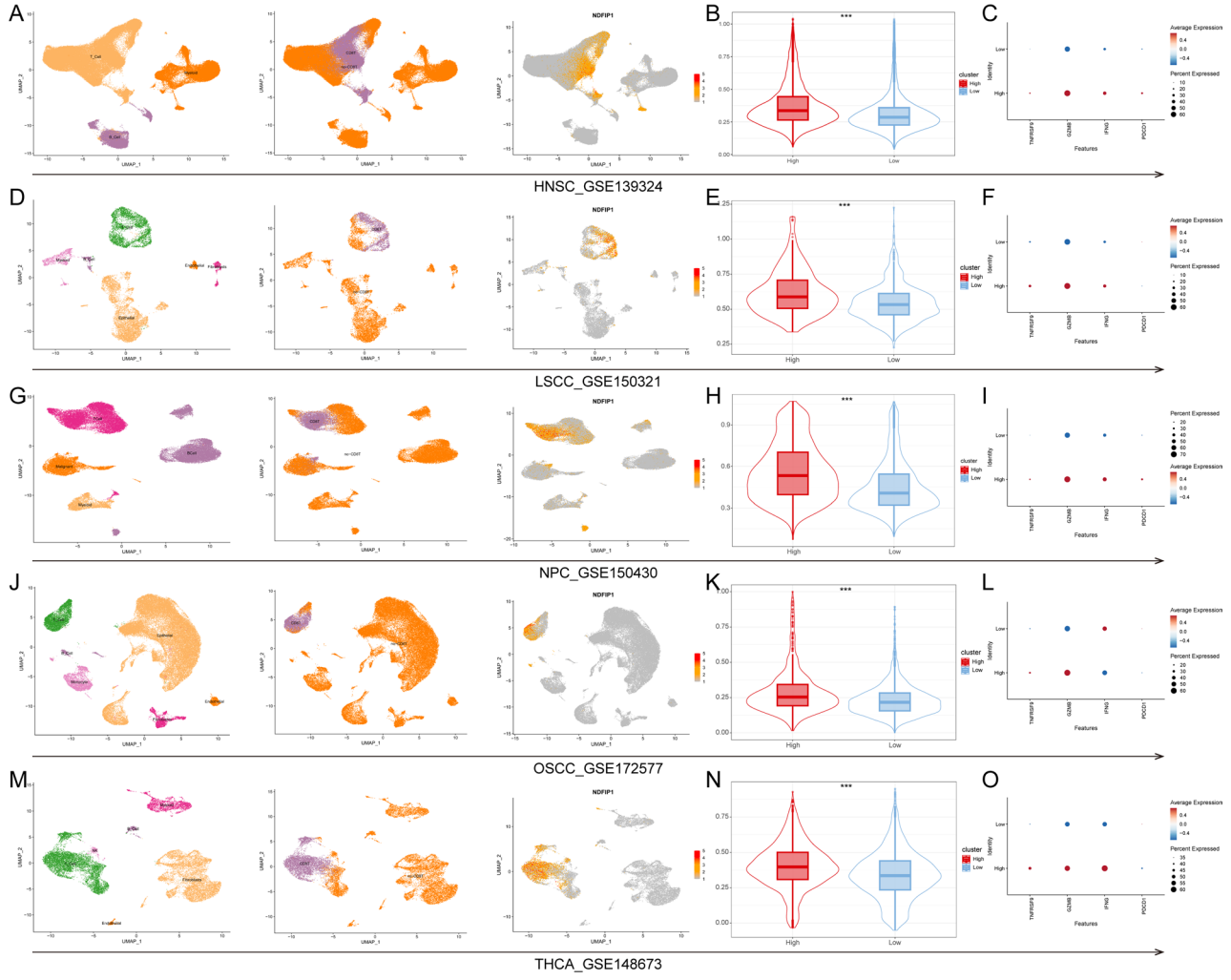

Fig. 8 Bioinformatics validation of NDFIP1.The UMAP plot shows the expression of NDFIP1 in single-cell data (Fig. 8a, d, g, j and m). The box plot presents the relationship between NDFIP1 and the oxidative phosphorylation pathway in CD8 T cells (Fig. 8b, e, h, k and n). The bubble plot presents the relationship between NDFIP1 and related genes (Fig. 8c, f, i, l and o)

phosphorylation scores were also higher in this group (Fig. 10B). Moreover, clinical data from multiple cohorts showed that higher NDFIP1 expression was associated with a greater likelihood of response to immune therapy (Fig. 10C). In summary, NDFIP1 enhances antitumor immune responses by regulating the oxidative phosphorylation pathway. Its high expression is associated with improved outcomes in immune therapy, highlighting its potential as a predictor of therapy efficacy. Moreover, we performed multiplex immunofluorescence staining on clinical pathological sections of head and neck squamous cell carcinoma (HNSC). The results indicated that patients in the non-responsive group to immunotherapy had fewer NDFIP1-positive CD8 + T cells compared to those in the responsive group (Fig. 10D).

Discussion

The importance of CD8 + T cells in tumor immunity is well established [15]. By creating a single-cell transcriptomic atlas of 53,660 CD8 + T cells, we conducted a detailed analysis of their heterogeneity and potential functions. This comprehensive atlas reveals distinct features of 11 stable CD8 + T cell clusters and highlights complex functional interactions between them. Notably, CCL5 + CD8+ T cells, the most abundant subset, primarily express CCL5 and GZMH, and are enriched in MHC class I and cytokine-receptor interaction pathways, confirming their central role in anti-tumor immunity [14]. Interestingly, the proportion of CCL5 + CD8+ T cells is reduced in metastatic sites, suggesting a more critical role for these cells in primary tumors. The TSTR (T cell stress response) subpopulation exhibited features consistent with previous studies, including high expression of HSPA1A and HSPA1B, and enrichment of the NF-κB and

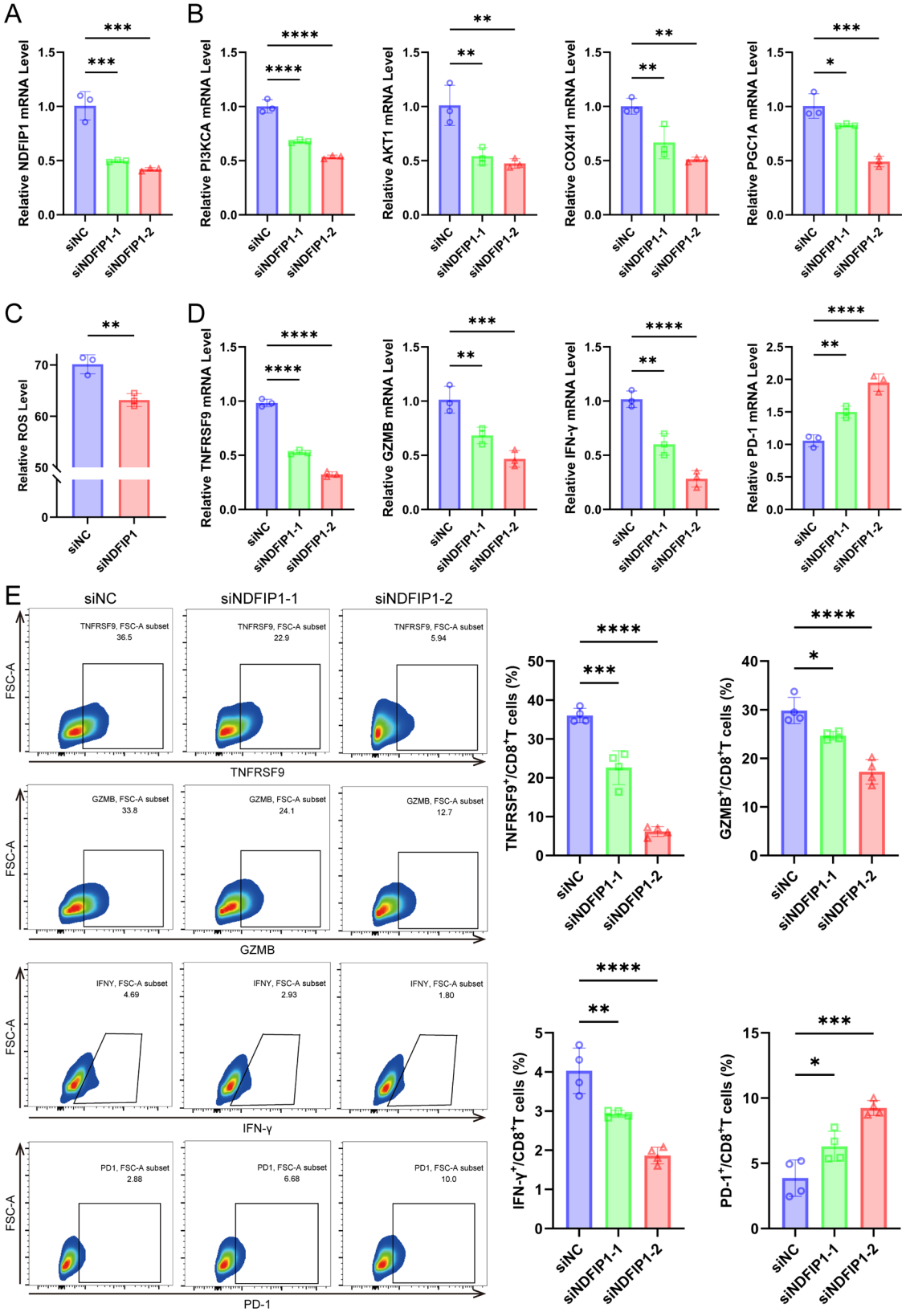

Fig. 9 Experimental validation of NDFIP1. (**a**) RT-PCR analysis of NDFIP1 mRNA expression after NDFIP1 knockout. (**b**) RT-PCR analysis of PI3KCA, AKT1, COX4I1, and PGC1A mRNA expression after NDFIP1 knockout. (**c**) Flow cytometry detection of ROS levels. (**d**) RT-PCR analysis of GZMB, IFN-γ, TNFRSF9, and PD-1 mRNA expression after NDFIP1 knockout. (**e**) Changes in GZMB, IFN-γ, TNFRSF9, and PD-1 were detected by flow cytometry after NDFIP1 knockout

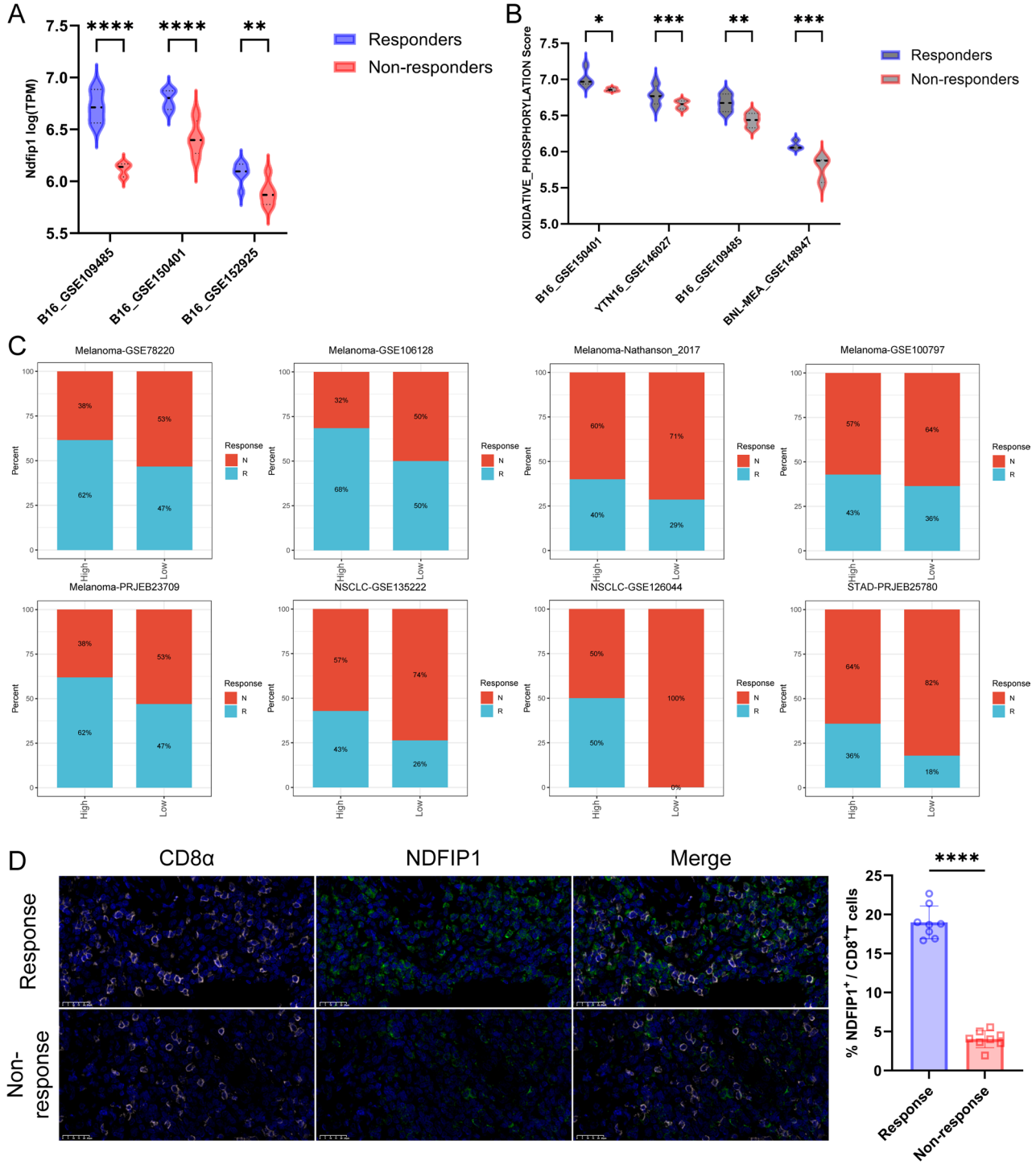

Fig. 10 The immunotherapeutic predictive potential of NDFIP1. **a**-**b** Compare gene or signature expression levels across different tumor models and ICB treatments, between responders and non-responders. **c** Chi-square test to evaluate the significance of the difference in immunotherapy response rates between high and low gene expression groups. **d** Representative image of immunofluorescence staining for immunostaining in the HNSC

PPAR signaling pathways, suggesting its potential role in coping with stress in the tumor microenvironment [16].

We also found an increase in PDCD1 + CD8+ T cells at the metastatic site, a finding that differs from previous studies [17, 18]. These cells predominantly expressed PDCD1 and LAG3 and were enriched for the JAK-STAT and PD-L1/PD-1 signaling pathways, suggesting that PDCD1 + CD8+ T cells may play a complex role in tumor metastasis involving immunosuppression and regulation of the tumor microenvironment. Cell communication

analysis revealed interactions between PDCD1 + CD8+ T cells and CCL5 + and CXCL13 + CD8+ T lymphocytes, suggesting functional crosstalk between different subpopulations.

Using a multi-model integration approach, we identified characteristic genes associated with PDCD1 + CD8+ T cells that have prognostic value in head and neck squamous cell carcinoma (HNSC) metastasis. Compared to single models, this integrated method improved gene selection accuracy and prognostic prediction stability by combining different algorithms. The StepCox[backward] + Ridge model achieved a 5-year AUC of 0.865, demonstrating outstanding performance in predicting outcomes. Five genes-PLS3, NDFIP1, MED15, JCHAIN, and FTH1-were consistently identified across multiple prognostic models. PLS3 is involved in cytoskeletal regulation [19], MED15 plays a role in transcriptional regulation [20], JCHAIN is linked to immunoglobulin formation [21], FTH1 is involved in iron metabolism and oxidative stress response [22], and NDFIP1 is downregulated in various cancers, particularly in HNSC. Although both NDFIP1 and MED15 were initially identified as highly expressed in $CD8^+$ T cells, their expression patterns in tumor versus adjacent normal tissues differed markedly. Notably, NDFIP1 expression was consistently reduced in tumor tissues, suggesting a potential loss of immune-regulatory function within the tumor microenvironment. In contrast, MED15 exhibited increased expression in tumor tissues compared with adjacent normal tissues, indicating that it may be more closely associated with tumor-intrinsic or pro-tumorigenic processes rather than $CD8^+$ T cell–mediated immune regulation. Given the focus of this study on identifying immune-related factors whose dysregulation in the tumor microenvironment may contribute to impaired antitumor $CD8^+$ T cell function, we therefore prioritized NDFIP1 for further investigation. The divergent tumor-associated expression patterns of NDFIP1 and MED15 highlight their potentially distinct biological roles in HNSCC and warrant separate mechanistic exploration in future studies.

In a pan-cancer analysis, we found that NDFIP1 is negatively correlated with tumor cell cycle and invasion/metastasis, while positively correlated with CD8 + T cell infiltration and immune pathways. Notably, NDFIP1 shows a strong positive correlation with the oxidative phosphorylation pathway, suggesting its role in regulating tumor metabolism. Although prior research focused on NDFIP1's functions in protein degradation and cell signaling [9, 23], our findings linking it to oxidative phosphorylation offer new insights into its role in tumor metabolism and immune regulation. Through multi-modal analyses of pan-cancer bulk transcriptomics, single-cell transcriptomics, and spatial transcriptomics, we confirmed NDFIP1's importance in immune regulation and prognosis. Given the central role of oxidative phosphorylation in energy metabolism and its strong link to tumor cell survival and proliferation, NDFIP1's association with this pathway highlights its potential role in metabolic regulation.

Our specific analyses showed that NDFIP1 expression is lower in HNSC tissues than in normal tissues. This finding, validated by paired and unpaired tests, immunohistochemistry, and single-cell data analysis, aligns with prior research supporting the widespread downregulation of NDFIP1 in various cancers [24, 25]. However, this study is the first to reveal a negative correlation between NDFIP1 downregulation and both clinical pathological stage and MKI67 expression in HNSC, suggesting that reduced NDFIP1 expression may be associated with tumor proliferation and clinical progression. This indicates NDFIP1 as a potential prognostic biomarker for HNSC. KEGG pathway enrichment analysis revealed that NDFIP1 expression is positively correlated with the oxidative phosphorylation pathway and negatively correlated with the steroid hormone biosynthesis pathway. This suggests that NDFIP1 may influence tumor growth and progression by modulating tumor cell metabolism through the oxidative phosphorylation pathway. The negative correlation with the steroid hormone biosynthesis pathway may reflect the role of NDFIP1 in hormone regulation, further illustrating its complex metabolic regulatory function.

Regarding immune regulation, we observed that high NDFIP1 expression was enriched in TNF and NF-κB signaling pathways, which is consistent with previous studies suggesting that NDFIP1 may regulate the tumor immune microenvironment through these pathways [26]. TNF signaling pathway plays a key role in immune cell recruitment and activation, while the NF-κB pathway is associated with inflammation and tumor invasiveness. Down-regulation of NDFIP1 may impair the function of these pathways, leading to immune evasion and tumor progression. Analysis of single-cell data further revealed a stable positive correlation between NDFIP1 and CD8 + T-cell infiltration, suggesting that NDFIP1 may influence immune responses by regulating CD8 + T-cell function. Specifically, the high NDFIP1 expression group was enriched in strong CD8 signaling and TCR diversity C2 (IFN-γ dominant) immune subtypes, whereas the low NDFIP1 expression group was enriched in high proliferative C1 (wound healing) subtypes with elevated angiogenic gene expression [27]. This suggests that NDFIP1 may influence the immune microenvironment by regulating CD8 + T cell infiltration and activity. Further analysis showed that elevated CTL levels in the high NDFIP1 expression group were associated with a better prognosis, whereas elevated CTL levels in the low NDFIP1 expression group were associated with a worse prognosis.

This suggests that NDFIP1 downregulation may be associated with T-cell depletion and immune evasion, which may affect the efficacy of immunotherapy. HPV status is a major determinant of the immune microenvironment in head and neck squamous cell carcinoma. Although HPV annotation was available for the TCGA-HNSCC cohort, the present study did not stratify analyses by HPV status, as the primary focus was to characterize immune cell–associated expression patterns of NDFIP1. Future studies incorporating HPV-stratified analyses and functional validation will be important to further delineate the context-dependent role of NDFIP1 in HNSCC.

Analysis of NDFIP1, oxidative phosphorylation, and TNFRSF9 showed that high expression of NDFIP1 was associated with active oxidative phosphorylation, and analysis of interactions with TNFRSF9 showed that patients with both low NDFIP1 and low TNFRSF9 expression had a poorer prognosis, whereas patients with high expression of both genes had a better prognosis. These findings suggest that NDFIP1 may regulate immune responses by modulating TNFRSF9 expression and play a key role in the tumor immune microenvironment. In addition, we found that NDFIP1 was upregulated in patients who responded to immunotherapy, and its expression was positively correlated with the likelihood of treatment response, further supporting its potential as a predictive biomarker for immunotherapy.

Conclusion

This study systematically reveals NDFIP1's critical role in head and neck squamous cell carcinoma (HNSC) and explores its relationship with metabolic and immune pathways, as well as immunotherapy response. For the first time, we demonstrate that NDFIP1 influences the tumor immune microenvironment and prognosis by modulating the oxidative phosphorylation pathway and immune-related signaling. These findings deepen our understanding of NDFIP1's function in cancer and provide new avenues for optimizing immunotherapy strategies in HNSC. Future studies should further explore NDFIP1's role in other cancers and assess its practical application as an immunotherapy biomarker.

Supplementary Information

The online version contains supplementary material available at https://doi.org/10.1186/s12935-026-04304-4.

Supplementary Material 1

Supplementary Material 2

Acknowledgements

We are very grateful for the data provided by databases such as TCGA, and GEO. Thanks to the reviewers and editors for their sincere comments.

Author contributions

YZ, DL, and LW performed study concept and design, revised the manuscript and make final approval of the version. JW analyzed data and wrote the manuscript. DX, ZC, DY, YT, YZ, and YS analyzed data, interpreted results. All authors read and approved the final paper.

Funding

This research was funded by the Natural Science Foundation of Changsha City, Hunan Province (No. kq2208490) and the Natural Science Foundation of Hunan Provincial (No. 2023JJ30068).

Data availability

The datasets analyzed during the current study are available from the corresponding and last author on reasonable request.

Declarations

Ethics approval

The ethics committee of Changsha Hospital of Traditional Chinese Medicine approved the present study (Number: 2024110702). Written consents were obtained from all patients.

Competing interests

The authors declare that the research was conducted in the absence of any commercial or financial relationships that could be construed as a potential conflict of interest.

Received: 14 September 2025 / Accepted: 9 April 2026
Published online: 16 April 2026

References

1. Johnson DE, et al. Head and neck squamous cell carcinoma. Nat Rev Dis Primers. 2020;6(1):92.
2. Sung H, et al. Global Cancer Statistics 2020: GLOBOCAN Estimates of Incidence and Mortality Worldwide for 36 Cancers in 185 Countries. CA Cancer J Clin. 2021;71(3):209–49.
3. Siegel RL, et al. Cancer statistics, 2023. CA Cancer J Clin. 2023;73(1):17–48.
4. Xia L, et al. The cancer metabolic reprogramming and immune response. Mol Cancer. 2021;20(1):28.
5. Koppenol WH, Bounds PL, Dang CV. Otto Warburg's contributions to current concepts of cancer metabolism. Nat Rev Cancer. 2011;11(5):325–37.
6. Zong WX, Rabinowitz JD, White E. Mitochondria Cancer Mol Cell. 2016;61(5):667–76.
7. Guo Y, et al. Metabolic reprogramming of terminally exhausted CD8(+) T cells by IL-10 enhances anti-tumor immunity. Nat Immunol. 2021;22(6):746–56.
8. Vardhana SA, et al. Impaired mitochondrial oxidative phosphorylation limits the self-renewal of T cells exposed to persistent antigen. Nat Immunol. 2020;21(9):1022–33.
9. Traeger L, et al. UBA6 and NDFIP1 regulate the degradation of ferroportin. Haematologica. 2022;107(2):478–88.
10. Mund T, Pelham HR. Regulation of PTEN/Akt and MAP kinase signaling pathways by the ubiquitin ligase activators Ndfip1 and Ndfip2. Proc Natl Acad Sci U S A. 2010;107(25):11429–34.
11. Yuan H, et al. CancerSEA: a cancer single-cell state atlas. Nucleic Acids Res. 2019;47(D1):D900–8.
12. Akbani R, et al. A pan-cancer proteomic perspective on The Cancer Genome Atlas. Nat Commun. 2014;5:3887.
13. Liu H, et al. ADORA1 inhibition promotes tumor immune evasion by regulating the ATF3-PD-L1 Axis. Cancer Cell. 2020;37(3):324–e3398.
14. Dangaj D, et al. Cooperation between Constitutive and Inducible Chemokines Enables T Cell Engraftment and Immune Attack in Solid Tumors. Cancer Cell. 2019;35(6):885–e90010.
15. Zheng L, et al. Pan-cancer single-cell landscape of tumor-infiltrating T cells. Science. 2021;374(6574):abe6474.
16. Chu Y, et al. Pan-cancer T cell atlas links a cellular stress response state to immunotherapy resistance. Nat Med. 2023;29(6):1550–62.
17. Fairfax BP, et al. Peripheral CD8(+) T cell characteristics associated with durable responses to immune checkpoint blockade in patients with metastatic melanoma. Nat Med. 2020;26(2):193–9.

18. Gros A, et al. PD-1 identifies the patient-specific CD8(+) tumor-reactive repertoire infiltrating human tumors. J Clin Invest. 2014;124(5):2246–59.
19. Zhong W, et al. The intricate mechanism of PLS3 in bone homeostasis and disease. Front Endocrinol (Lausanne). 2023;14:1168306.
20. Hua X, et al. MED15 is upregulated by HIF-2alpha and promotes proliferation and metastasis in clear cell renal cell carcinoma via activation of SREBP-dependent fatty acid synthesis. Cell Death Discov. 2024;10(1):188.
21. Li Y, et al. Structural insights into immunoglobulin M. Science. 2020;367(6481):1014–7.
22. Fang Y, et al. Inhibiting Ferroptosis through Disrupting the NCOA4-FTH1 Interaction: A New Mechanism of Action. ACS Cent Sci. 2021;7(6):980–9.
23. Wang Y, Tong X, Ye X. Ndfip1 negatively regulates RIG-I-dependent immune signaling by enhancing E3 ligase Smurf1-mediated MAVS degradation. J Immunol. 2012;189(11):5304–13.
24. Cheng Y, et al. NDFIP1 limits cellular TAZ accumulation via exosomal sorting to inhibit NSCLC proliferation. Protein Cell. 2023;14(2):123–36.
25. Howitt J, et al. Ndfip1 represses cell proliferation by controlling Pten localization and signaling specificity. J Mol Cell Biol. 2015;7(2):119–31.
26. Xu H, et al. Iron status and lipopolysaccharide regulate Ndfip1 by activation of nuclear factor-kappa B. Biometals. 2013;26(6):981–8.
27. Thorsson V, et al. The Immune Landscape of Cancer. Immunity. 2018;48(4):812–e83014.

Publisher's note